Journal of Nuclear Materials 455 (2014) 640–644

Contents lists available at ScienceDirect

Journal of Nuclear Materials

journal homepage: www.elsevier.com/locate/jnucmat

Creep deformation and rupture behavior of CLAM steel at 823 K and 873 K

Boyu Zhong [a], Bo Huang [a,*], Chunjing Li [a], Shaojun Liu [a], Gang Xu [a], Yanyun Zhao [a,b], Qunying Huang [a,b]

[a] Key Laboratory of Neutronics and Radiation Safety, Institute of Nuclear Energy Safety Technology, Chinese Academy of Sciences, Hefei, Anhui 230031, China
[b] University of Science and Technology of China, Hefei, Anhui 230027, China

ARTICLE INFO

Article history:
Available online 30 August 2014

ABSTRACT

China Low Activation Martensitic (CLAM) steel is selected as the candidate structural material in Fusion Design Study (FDS) series fusion reactor conceptual designs. The creep property of CLAM steel has been studied in this paper. Creep tests have been carried out at 823 K and 873 K over a stress range of 150–230 MPa. The creep curves showed three creep regimes, primary creep, steady-state creep and tertiary creep. The relationship between minimum creep rate ($\dot{\varepsilon}_{min}$) and the applied stress (σ) could be described by Norton power law, and the stress exponent n was decreased with the increase of the creep temperature. The creep mechanism was analyzed with the fractographes of the rupture specimens which were examined by scanning electron microscopy (SEM). The coarsening of precipitates observed with transmission electron microscope (TEM) indicated the microstructural degradation after creep test.

1. Introduction

With the characteristics of inherent void swelling resistance, better thermo-physical and thermo-mechanical properties compared to the austenitic stainless steels, Reduced Activation Ferritic/Martensitic (RAFM) steels have been selected as the primary candidate structural materials for the demonstration fusion reactor and future fusion power plant [1]. As one of the RAFM steels, CLAM steel has been developed at the Institute of Nuclear Energy Safety Technology (INEST), Chinese Academy of Sciences (CAS), under wide collaboration with many institutes and universities both indigenous and overseas [2]. A series of R&D activities on CLAM steel has been carried out. These activities mainly cover physical and mechanical properties [3–7], fabrication techniques of test blanket module (TBM) [8,9], irradiation properties and activation analysis etc. [10,11].

CLAM steel is considered as the primary candidate structural material for dual functional lithium lead (DFLL) blanket of FDS series fusion reactor conceptual design [12,13] and the ITER China TBM [14–16]. The evaluation of mechanical properties of CLAM steel is urgently required, especially the behavior of CLAM steel under long-term loading conditions at the elevated operating temperatures due to the extreme service conditions of the fusion blanket in fusion reactor. Therefore, it is necessary to evaluate the creep property of CLAM steel and define the service life of the CLAM components in the TBM.

In this paper, the creep deformation and rupture behavior of CLAM steel at 823 K and 873 K in air were studied to evaluate and analyze the creep property of CLAM steel and its microstructural evolution during creep.

2. Experimental

The material used in this study was CLAM steel (HEAT 0912), an ingot of 1.2 ton, melted by vacuum induction furnace. The ingot was hot rolled into plates with different thickness and its chemical composition was given in Table 1 [2]. Then, these plates were normalized to obtain complete martensite. The heat treatment was as follows: austenitizing at 1253 K for 30 min followed by air cooling and then tempering at 1033 K for 90 min followed by air cooling. The cylindrical creep specimens with 50 mm in gauge length and 5 mm in diameter were machined from the CLAM plate with the thickness of 36 mm.

The creep rupture tests with constant load were performed at 823 K and 873 K in air over a stress range of 150–230 MPa with uniaxial creep test machines according to the standard of ISO 204-2009. The deviation of experimental temperature was controlled within ±2 K. The elongation of the specimens was measured with a linear encoder. The microstructure observation of the specimens was carried out with optical microscope (OM), scanning electron microscope (SEM) and transmission electron microscope (TEM). For further analysis of the precipitates, selected area

* Corresponding author. Tel.: +86 0551 65592157; fax: +86 0551 65591397.
E-mail address: bo.huang@fds.org.cn (B. Huang).

http://dx.doi.org/10.1016/j.jnucmat.2014.08.041
0022-3115/

Table 1
Chemical compositions of CLAM (HEAT 0912) (wt.%).

Element	Content
Cr	8.86
C	0.094
W	1.48
V	0.21
Ta	0.12
Mn	0.48
Ti	<0.005
S	0.0023
P	0.004
Al	<0.01
Fe	Balance

electron diffraction (SAED) and energy dispersive spectroscopy (EDS) were also used.

3. Result and discussion

3.1. Microstructure of as-received steel

The as-received CLAM steel was classic tempered martensite, as shown in Fig. 1. The dimension of prior austenite grain was measured to be about 10 μm. The size of lath structure with high dislocation density ranged from 0.2 μm to 0.3 μm (as seen in Fig. 1(c)). One of the main strengthening mechanisms of the CLAM steel is precipitation hardening. There are two types of precipitates: Cr-rich $M_{23}C_6$ and Ta-rich or V-rich MX particles, where M represents alloying elements, such as Cr, V, Ta and X represents C or N. The $M_{23}C_6$ precipitates with the size of 100–150 nm mainly distributed at the prior austenite grain boundaries and the martensitic lath boundaries, while near-spherical MX particles with the size of 40–50 nm mainly located in the matrix [5]. The EDS results (as shown in Fig. 2) revealed that $M_{23}C_6$ carbides were Cr-rich precipitates and MX particles were Ta-rich precipitates. The thermal stability of the fine MX precipitates led to the increase of the long-term creep resistance [17].

3.2. Creep deformation

A creep curve is normally characterized by primary (or transient), secondary (or steady-state) and tertiary (or accelerated creep) stages [18]. The strain (ε) versus time (t) curves of CLAM steel at various stress level at 823 K and 873 K are shown in Fig. 3. And the creep test at 150 MPa at 873 K is still undergoing. The rupture life of CLAM steel decreased with the increase of the stress at the same temperature and the rupture life of CLAM steel was similar to other RAFMs at the same condition [19]. The results showed that higher stress made the creep deformation of CLAM steel experience with relatively shorter transient regime followed by an extended acceleration regime with actually no secondary regime. The steady-state regime was found on the condition of lower stress. The change of the creep rate in CLAM steel could be explained by the climb controlled motion of dislocations. It could be described by the capacity of strain hardening and the dislocation recovery. With the increase of the strain, the creep rate reduced in the transient creep regime because of the strain hardening effect caused by the dislocation multiplication and interaction. In the steady-state regime, the creep rate was stabilized as the effect of strain hardening was counteracted by the dislocation annihilation and rearrangement. At the acceleration regime, the creep rate increased due to the growth and coalescence of creep cavities.

Generally, the relationship between minimum creep rate ($\dot{\varepsilon}_{min}$) and the applied stress (σ) could be described by Norton creep law with the form [20]:

$$\dot{\varepsilon}_{min} = A\sigma^n$$

where A is a constant and n is the stress exponent. The result of the minimum creep rate ($\dot{\varepsilon}_{min}$) versus the applied stress (σ) of CLAM steel is shown in Fig. 4. It was found that the stress exponent n was temperature dependent and reduced from 19 to 15 with the

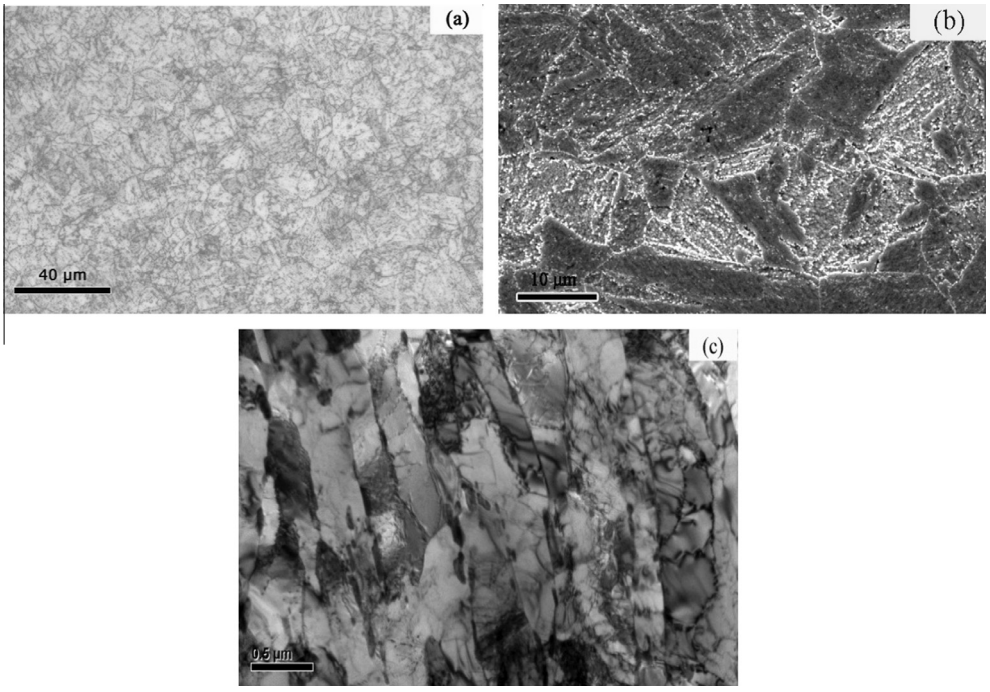

Fig. 1. (a) An optical micrograph showing the tempered microstructure, (b) an SEM micrograph showing the precipitates and (c) a TEM micrograph showing the lath structure.

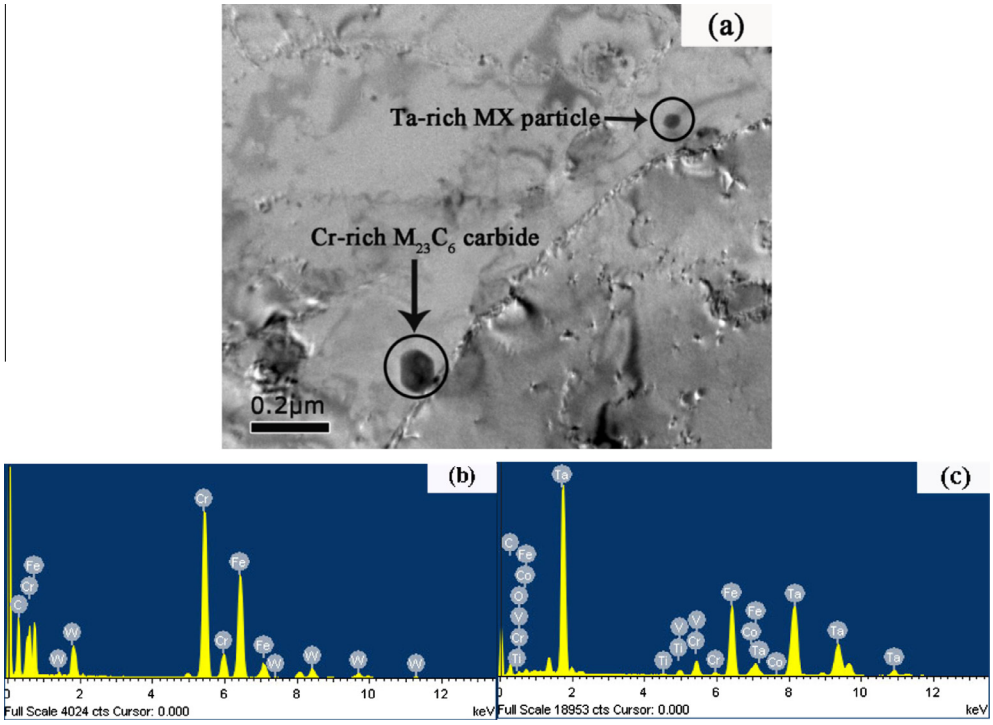

Fig. 2. (a) Precipitates in CLAM specimens; EDS analysis of the precipitates in CLAM specimens, (b) Cr-rich $M_{23}C_6$ carbide and (c) Ta-rich MX particle.

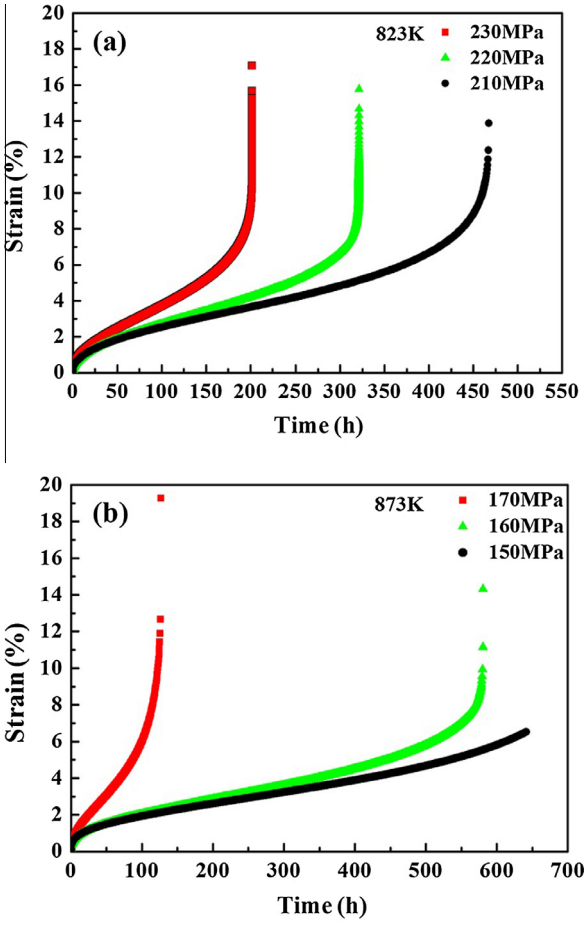

Fig. 3. Experimental creep curves of CLAM steel at different stress levels at (a) 823 K and (b) 873 K.

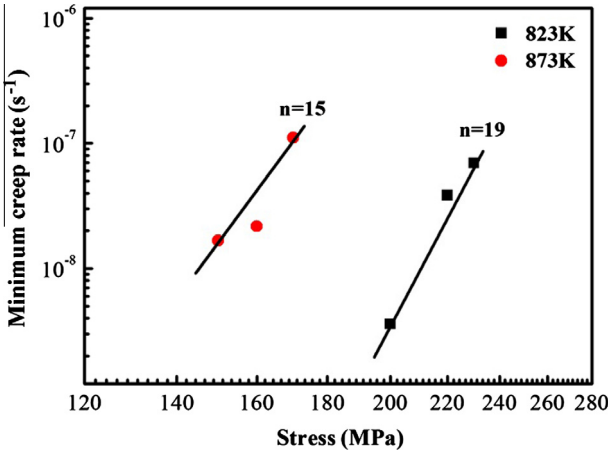

Fig. 4. Minimum creep rate versus applied stress for CLAM steel at 823 K and 873 K.

increase of the temperature from 823 K to 873 K. The reduction in n with the elevation of the temperature was also found in Eurofer97 [19] and other 9–12 wt.% Cr steel [21–24]. The decrease of n indicated a change in creep deformation mechanism [17]. When the creep is controlled by dislocation process, the stress exponent n is usually equal to 4–7, as proved in many pure metals and single-phase alloys displaying normal creep curves at high temperatures. In addition, in the alloys which were strengthened by fine precipitates, the value of n was obviously greater than the material without precipitated particles. While the creep deformation was non-dislocation based diffusional creep at very low stresses and high temperatures such as $T \approx T_m$, n would reduce to about 1. The high value of n in CLAM steel at 823 K and 873 K might indicate that the creep behavior was controlled by dislocation movement and the steel was strengthened by dispersed precipitates.

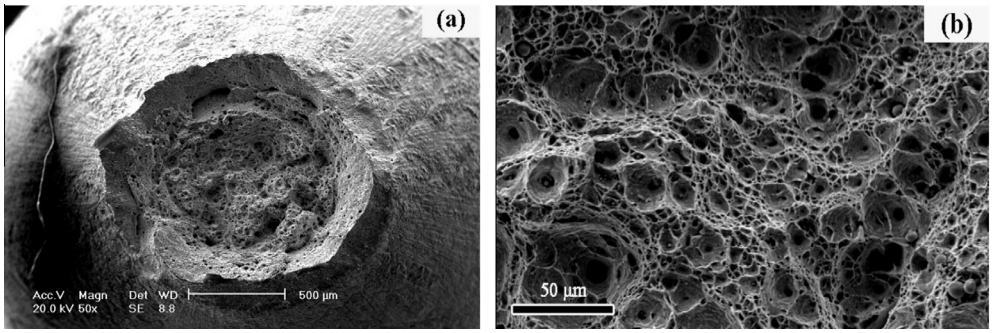

Fig. 5. (a) Necking regions and (b) facture surface of the specimen tested at 210 MPa and 823 K.

3.3. Creep rupture behavior

The fractographes of the specimens examined by SEM are shown in Fig. 5. The character of dimples owing to the coalescence of microvoids indicated the occurrence of transgranular fracture under all the test conditions. Similar fracture morphologies were also observed in other 9 wt.% Cr martensitic steel e.g. Grade 91 [25] and India RAFM steel [26]. The variation of elongation as a function of rupture life for CLAM steel is shown in Fig. 6. The creep ductility values remained reasonably high at all test temperatures and a marginal loss of ductility was observed with the increase of the rupture life.

External necking and reduction in the cross-section of CLAM specimens were observed when the creep specimens ruptured (Fig. 5(a)). The load bearing lateral section of CLAM steel decreased obviously during long time creep tests. There was no specimen necking to a point, which indicated that internal damage had a significant effect on material failure. Therefore, internal necking caused by the degradation of the microstructure and voids formation, growth and coalescence should be taken into consideration to explain the creep failure mechanism in CLAM steel. In generally, the nucleation and growth of cavity always take place throughout the whole creep deformation process. However, the pace would be accelerated in the tertiary stage.

3.4. The changes of microstructure after creep

The microstructure of CLAM steel after creep deformation at 823 K for 1559 h is shown in Fig. 7. It was found that the microstructure of CLAM steel was degraded after long time creep deformation. The size, morphology and distribution of precipitates were the main microstructure changes during creep [27]. Coarsening of $M_{23}C_6$ carbides on the prior austenite grain boundaries was observed on creep exposure. It was shown that the size of the $M_{23}C_6$ carbides had coarsened to about 200 nm after 1595 h of creep exposure at 823 K. As the MX precipitates were more thermally stable than $M_{23}C_6$ precipitates and hardly grew during high-temperature creep [28,29], the particle size of MX precipitates showed no obvious change.

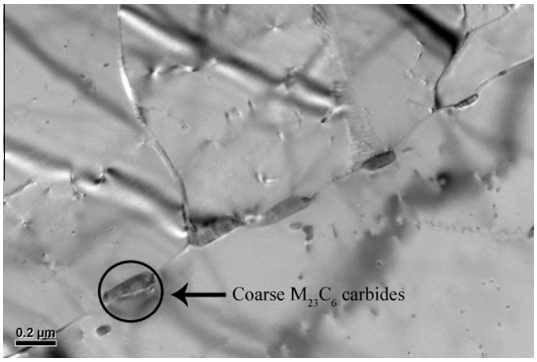

Fig. 7. Coarse $M_{23}C_6$ carbides on subgrain boundaries after creep test at 873 K for 1595 h.

CLAM steel was strengthened by $M_{23}C_6$ and MX precipitates. The $M_{23}C_6$ precipitates on the prior austenite grain boundaries constituted an obstacle to dislocation movement, while the coarsening of $M_{23}C_6$ particles would lead to less obstacles and easier

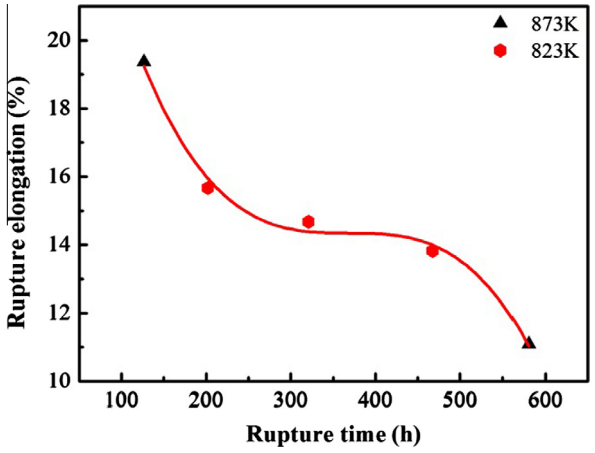

Fig. 6. Variation of rupture life versus rupture elongation at 823 K and 873 K of CLAM steel.

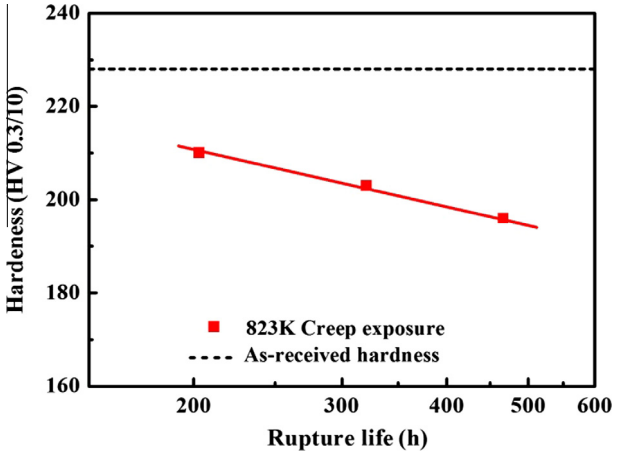

Fig. 8. Variation in hardness of CLAM steel after creep test at 823 K.

movement of the dislocations, thus the evolution of the microstructure would be accelerated and finally result in the reduction of mechanical strength. The hardness of creep specimens near the fracture surface was measured. The Vickers hardness results after creep test at 873 K were given in Fig. 8, which indicated that the hardness of CLAM steel after creep test was reduced as a result of accelerated microstructure deterioration.

4. Conclusions

The creep deformation and rupture behavior of CLAM steel were studied at 823 K and 873 K over a stress range of 150–230 MPa. The detailed results are as follows:

(1) The relationship between minimum creep rate and stress obeyed the Norton power law and revealed high values of stress exponent. The stress exponent decreased with the increase of the experimental temperature.
(2) The fracture behavior of CLAM steel was transgranular fracture characterized by dimples resulting from the coalescence of microvoids.
(3) Microstructure degradation was observed after long time creep deformation. The coarsened $M_{23}C_6$ precipitates played an important role in the reduction of mechanical strength.

Acknowledgements

This work was supported by the China National Natural Science Foundation with Grant No. 51101148, the Special Foundation of President of Hefei Institutes of Physical Science with Grant No. YZJJ201326, the National Basic Research Program of China with Grant Nos. 2011GB108001, 2011GB113001, 2013GB108005 and 2014GB112003.

References

[1] N. Baluc, D. Gelles, S. Jitsukawa, A. Kimura, R. Klueh, G. Odette, et al., J. Nucl. Mater. 367–370 (2007) 33–41.
[2] Q. Huang, C. Li, Y. Li, M. Chen, M. Zhang, L. Peng, et al., J. Nucl. Mater. 367–370 (2007) 142–146.
[3] Q. Huang, N. Baluc, Y. Dai, S. Jitsukawa, A. Kimura, J. Konys, et al., J. Nucl. Mater. 442 (2013) S2–S8.
[4] Y. Li, Q. Huang, Y. Wu, T. Nagasaka, T. Muroga, J. Nucl. Mater. 367–370 (2007) 117–121.
[5] S. Liu, Q. Huang, L. Peng, Y. Li, C. Li, Fusion Eng. Des. 879 (2012) 1628–1632.
[6] Q. Wu, S. Zheng, Q. Huang, S. Liu, Y. Han, J. Nucl. Mater. 442 (2013) S67–S70.
[7] S. Zheng, Q. Wu, Q. Huang, S. Liu, Y. Han, Fusion Eng. Des. 86 (2011) 2616–2619.
[8] B. Huang, Q. Huang, C. Li, S. Liu, Q. Wu, Fusion Eng. Des. 86 (2011) 2602–2606.
[9] C. Li, Q. Huang, P. Zhang, J. Nucl. Mater. 386–388 (2009) 550–552.
[10] L. Peng, Q. Huang, C. Li, S. Liu, J. Nucl. Mater. 386–388 (2009) 312–314.
[11] L. Peng, Q. Huang, S. Ohnuki, C. Yu, Fusion Eng. Des. 86 (2011) 2624–2626.
[12] Y. Wu, Fusion Eng. Des. 81 (2006) 2713–2718.
[13] Y. Wu, Fusion Eng. Des. 83 (2008) 1683–1689.
[14] Y. Wu, J. Nucl. Mater. 367–370 (2007) 1410–1415.
[15] Y. Wu, Nucl. Fusion 47 (2007) S1533–S1539.
[16] Y. Wu, Fusion Eng. Des. 82 (2007) 1893–1903.
[17] M. Tamura, H. Sakasegawa, A. Kohyama, H. Esaka, K. Shinozuka, J. Nucl. Mater. 321 (2003) 288–293.
[18] M.E. Kassner, Fundamentals of Creep in Metals and Alloys, second ed., Elsevier, Amsterdam, 2008.
[19] P. Fernández, A. Lancha, J. Lapeña, R. Lindau, M. Rieth, M. Schirra, Fusion Eng. Des. 75 (2005) 1003–1008.
[20] F.H. Norton, The Creep of Steel at High Temperatures, McGraw-Hill, New York, 1929.
[21] B. Choudhary, E. Isaac Samuel, J. Nucl. Mater. 412 (2011) 82–89.
[22] K. Sawada, K. Kubo, F. Abe, Mater. Sci. Eng. A 319 (2001) 784–787.
[23] F. Abe, Mater. Sci. Eng. A 319 (2001) 770–773.
[24] K. Kimura, K. Sawada, H. Kushima, Trans. Ind. Inst. Met. 63 (2010) 123–129.
[25] T. Shrestha, M. Basirat, I. Charit, G.P. Potirniche, K.K. Rink, Mater. Sci. Eng. A 565 (2013) 382–391.
[26] J. Vanaja, K. Laha, R. Mythili, K. Chandravathi, S. Saroja, M. Mathew, Mater. Sci. Eng. A 533 (2012) 17–25.
[27] P. Ennis, A. Czyrska-Filemonowicz, Sadhana 28 (2003) 709–730.
[28] M. Taneike, K. Sawada, F. Abe, Metall. Mater. Trans. A 35 (2004) 1255–1262.
[29] M. Tamura, H. Kusuyama, K. Shinozuka, H. Esaka, J. Nucl. Mater. 367–370 (Part A) (2007) 137–141.